

Original Article

# Activation of transient receptor potential vanilloid 3 is required for keratinocyte differentiation and epidermal barrier formation

Elina Da Sol Chung<sup>1,#</sup>, Yu Ran Nam<sup>2,#</sup>, Hyun Jong Kim<sup>2,3,#</sup>, Young Keul Jeon<sup>1</sup>, Kyung Sun Park<sup>4</sup>, Woo Kyung Kim<sup>2,5,\*</sup>, Sung Joon Kim<sup>1,4,\*</sup>, and Joo Hyun Nam<sup>2,3,\*</sup>

<sup>1</sup>Department of Biomedical Sciences, Seoul National University College of Medicine, Seoul 03080, Korea, <sup>2</sup>Channelopathy Research Center (CRC), Dongguk University College of Medicine, Goyang 10326, Korea, <sup>3</sup>Department of Physiology, Dongguk University College of Medicine, Gyeongju 38066, Korea, <sup>4</sup>Wide River Institute of Immunology, Seoul National University College of Medicine, Hongcheon 25159, Korea, <sup>5</sup>Department of Internal Medicine, Dongguk University Graduate School of Medicine, Goyang 10326, Korea

## ARTICLE INFO

Received October 4, 2024  
Revised February 19, 2025  
Accepted March 7, 2025  
Published online April 28, 2025

### \*Correspondence

Woo Kyung Kim  
E-mail: wk2kim@naver.com  
Sung Joon Kim  
E-mail: sjoonkim@snu.ac.kr  
Joo Hyun Nam  
E-mail: jhnam@dongguk.ac.kr

### Key Words

Cell differentiation  
Inflammation  
Keratinocytes  
Skin physiology  
TRPV cation channels

#These authors contributed equally to this work.

**ABSTRACT** Transient receptor potential vanilloid 3 (TRPV3)-mediated Ca<sup>2+</sup> signaling in keratinocytes plays a crucial role in epidermal keratinocyte differentiation and triggers the release of pro-inflammatory cytokines, causing inflammation and itching. However, the regulation of skin barrier recovery by TRPV3 and its expression during keratinocyte differentiation remain unexplored. This study aimed to investigate the role and expression levels of TRPV3 in keratinocyte differentiation and skin barrier recovery, focusing on the effects of varying TRPV3 activation using pharmacological agents. Differentiation of primary human keratinocytes was induced in high-calcium media, and TRPV3 activity and expression were assessed using patch-clamp, fura-2 fluorimetry, and immunoblotting. The effects of TRPV3 agonists on skin barrier recovery following tape stripping were evaluated by measuring transepidermal water loss in mice. Results showed that TRPV3 expression, current density, and agonist-induced [Ca<sup>2+</sup>]<sub>i</sub> changes increased with keratinocyte differentiation. The TRPV3 antagonist, ruthenium red, inhibited both keratinocyte differentiation and TRPV3 upregulation. TRPV3 agonists (2-APB/carvacrol) facilitated early differentiation but paradoxically downregulated TRPV3 expression at higher concentrations. Moderate TRPV3 activation by lower agonist concentrations enhanced skin barrier recovery, while higher concentrations hindered recovery and induced immune cell infiltration. These findings highlight the dual role of TRPV3 in skin homeostasis and suggest that targeted modulation of TRPV3 could be a promising strategy for treating skin disorders.

## INTRODUCTION

Keratinocytes formed in the basal layer of the epidermis undergo a series of changes known as keratinization. Calcium gradients in the skin are crucial for the differentiation process. Keratinocytes of the basal layer are proliferating in the low level of extracellular Ca<sup>2+</sup> ([Ca<sup>2+</sup>]<sub>e</sub>), and the higher [Ca<sup>2+</sup>]<sub>i</sub> in the upper

epidermis triggers the differentiation phenotypes including the increased keratin 1 (K1) and loricrin (LRC) along with the decreased keratin 14 (K14) [1-5]. The Ca<sup>2+</sup>-induced differentiation of keratinocytes and the formation of a skin barrier is essential for maintaining skin hydration [6,7].

Transient receptor potential vanilloid 3 (TRPV3) is a non-selective cation channel that is highly expressed in epidermal



This is an Open Access article distributed under the terms of the Creative Commons Attribution Non-Commercial License, which permits unrestricted non-commercial use, distribution, and reproduction in any medium, provided the original work is properly cited. Copyright © Korean J Physiol Pharmacol, pISSN 1226-4512, eISSN 2093-3827

**Author contributions:** E.D.S.C. performed formal analysis, investigation, visualization and wrote the original draft. Y.R.N., H.J.K., and Y.K.J. performed formal analysis, investigation, and visualization. K.S.P. conducted formal analysis, investigation, and provided resources. W.K.K. conceptualized the study, supervised, managed project administration, and reviewed and edited the manuscript. S.J.K. conceptualized the study, reviewed and edited the manuscript, and managed project administration. J.H.N. conceptualized the study, wrote the original draft, supervised, managed project administration, and reviewed and edited the manuscript.

keratinocytes [8,9]. TRPV3 is activated by innocuous warm temperatures (33°C–39°C) and a variety of chemical agonists, such as 2-aminoethoxydiphenyl borate (2-APB), carvacrol and intracellular protons [10–13]. Activation of TRPV3 can lead to the sensation of temperature, pain, and itch in the skin [14–23]. TRPV3 mediates calcium influx, triggering intracellular calcium ( $[Ca^{2+}]_i$ ) signaling in keratinocytes, which plays a crucial role in skin homeostasis such as skin barrier function and hair growth [24–26].

TRPV3 has been suggested as a part of the signaling complex with the epidermal growth factor receptor (EGFR) which is essential for the differentiation of keratinocytes, hair morphogenesis, and skin barrier maintenance [27]. The activation of the EGFR signaling pathway downstream of TRPV3-mediated calcium influx has been implicated in the pro-proliferative and pro-migratory effects [28,29]. The importance of TRPV3 for skin health is underscored by the Olmstead syndrome with a loss/gain of function mutations in TRPV3. The Olmsted syndrome patients with gain-of-function mutation showed palmoplantar and periorificial keratoderma, alopecia, and severe itching [30–33].

On the other hand, excessive TRPV3 activation has been linked to the pathogenesis of inflammatory skin conditions, such as atopic dermatitis. Increased TRPV3 expression and activity in keratinocytes can lead to the production of pro-inflammatory cytokines (e.g., interleukin (IL)-1 $\alpha$ , IL-6, IL-8, TNF- $\alpha$ ) with a development of itch sensation [34,35]. The complicated findings suggest that TRPV3 activity in keratinocytes requires tight regulation to maintain proper calcium homeostasis and cellular functions.

Despite the findings indicating the role of TRPV3 in skin physiology, the level of TRPV3 expression in differentiating keratinocytes has not been elucidated yet. Furthermore, the potential dual effects of TRPV3 activation on skin barrier recovery and inflammation have not been systematically investigated *in vivo*.

In this study, we aim to address these knowledge gaps by investigating TRPV3 expression and its functional correlation with keratinocyte differentiation markers in primary human keratinocytes. Additionally, we employ a mouse model with skin barrier disruption to evaluate the effects of TRPV3 modulation on skin barrier recovery and inflammation.

## METHODS

### Cell culture

Normal human epidermal keratinocytes (Cat. No. 00192627, LONZA) were cultured in Keratinocyte Growth Medium BulletKit (KGM, LONZA) containing low calcium (0.05–0.15 mM). Cells were maintained at 37°C in a humidified atmosphere of 5% CO<sub>2</sub>. The cells were passaged when they reached 70%–80% confluence, and only passages 1–3 were used for experiments to ensure consistent cell behavior. For differentiation studies,

keratinocytes were seeded at a density of  $2.5 \times 10^4$  cells/cm<sup>2</sup> and cultured until reaching 80% confluence. Differentiation was then induced by switching to high-calcium medium (1.3 mM Ca<sup>2+</sup>) for up to 5 days, with medium changes every 48 h [4,36].

### Electrophysiology

Whole-cell (w-c) patch-clamp recordings were performed at room temperature (~21°C–23°C). The internal solution contained 140 mM CsCl, 1 mM MgCl<sub>2</sub>, 10 mM HEPES, and 10 mM BAPTA (pH 7.2, titrated with CsOH) without MgATP. The bath solution contained 140 mM NaCl, 5 mM KCl, 2 mM CaCl<sub>2</sub>, 1 mM MgCl<sub>2</sub>, 10 mM HEPES, and 10 mM glucose (pH 7.4, titrated with NaOH). Both CaCl<sub>2</sub> and MgCl<sub>2</sub> were omitted to prepare the divalent-free bath solution. The data were collected using an Axopatch 200A patch clamp amplifier, Digidata 1440A, and pCLAMP 10.7 software (Axon Instruments). w-c currents were digitized at 10 kHz and low pass filtered at 2 kHz. The recorded data were analyzed with pCLAMP 10.7 and Origin 2021b (OriginLab).

Conventional w-c patch clamp recordings of TRPV3 in primary human keratinocytes. w-c currents were generated in response to 200 ms voltage ramps from –100 to +100 mV, applied every 20 sec, with a holding potential at –60 mV.

### Calcium imaging

$[Ca^{2+}]_i$  measurements were performed using the fluorescent Ca<sup>2+</sup> indicator Fura-2 acetoxymethyl ester (Fura-2 AM; Thermo Fisher Scientific). Primary human keratinocytes cultured on flame-sterilized coverslips were loaded with Fura-2 AM (2  $\mu$ M) in normal Tyrode's solution (145 mM NaCl, 10 mM HEPES, 5 mM glucose, 3.6 mM KCl, 2 mM CaCl<sub>2</sub>, and 1 mM MgCl<sub>2</sub>; pH 7.4, titrated with NaOH). Coverslips with the loaded cells were mounted in a chamber on an inverted microscope (Nikon Eclipse Ti; Nikon) and alternately exposed to excitation wavelengths of 340 nm (100 ms) and 380 nm (30 ms), with emission recorded at 510 nm. Fluorescence was excited using a pE-340 fura illuminator (CoolLED; Andover) and recorded with a sCMOS pco.edge 4.2 camera (PCO). Image acquisition and analysis were performed using NIS-Element AR Version 5.00.00 software (Nikon). The ratio of fluorescence intensities at 340 nm and 380 nm (F340/F380) was used as an indicator of  $[Ca^{2+}]_i$ .

### Immunoblot assay

The total lysates of primary human keratinocytes were collected and diluted in a SDS sample buffer and boiled for denaturation. The purified proteins were separated by SDS-PAGE and transferred to PVDF membranes. The membranes were blocked with either 10% skim milk or bovine serum albumin in phosphate-buffered saline with Tween 20 (PBST) and incubated with anti-TRPV3, K1, K14, LRC, or GAPDH antibody in

PBST. Detection was carried out using peroxidase-conjugated anti-rabbit or anti-mouse secondary antibody with an enhanced chemiluminescence reagent (Amersham Pharmacia Biotech, GE Healthcare).

## Histology and staining

Mouse skin tissues were fixed in 4% paraformaldehyde at 4°C for 3 h and then embedded in paraffin. Paraffin-embedded sections were stained with hematoxylin and eosin (H&E). For immune cell infiltration analysis, paraffin blocks were prepared from two dorsal skin sites of three animals per group. Photomicrographs were taken using a bright-field microscope (Nikon) at 400× magnification. One section from each block was analyzed, yielding 6 images per group (2 sections per animal, 3 animals per group). Immune cells were manually counted in six random fields per section by a blinded observer to reduce bias.

## Barrier recovery test

Balb/c female mice were purchased from Orient Bio and housed according to the IACUC guidelines of Dongguk University (2019–09190). Previous studies indicate that TRPV3, when endogenously expressed, is more effectively activated by a combination of agonists than by a single agonist [19,20]. Based on this, two concentrations of TRPV3 agonist cocktails were prepared (300 μM carvacrol + 30 μM 2-APB, 3,000 μM carvacrol + 300 μM 2-APB) in Dulbecco's phosphate-buffered saline. Female BALB/c mice (8 weeks old) had their dorsal hair shaved, and 96 h later, their dorsal skin was tape-stripped to achieve a transepidermal water loss (TEWL) of ~140 g/(m<sup>2</sup>·h). Following this, 100 μl of each agonist, antagonist, or the vehicle (0.02% dimethyl sulfoxide) was applied to the skin and covered with plastic wrap for 15 min to aid absorption. TEWL was measured at 0, 1, 3, 6, 10, 24, and 30 h after barrier disruption. Environmental conditions were main-

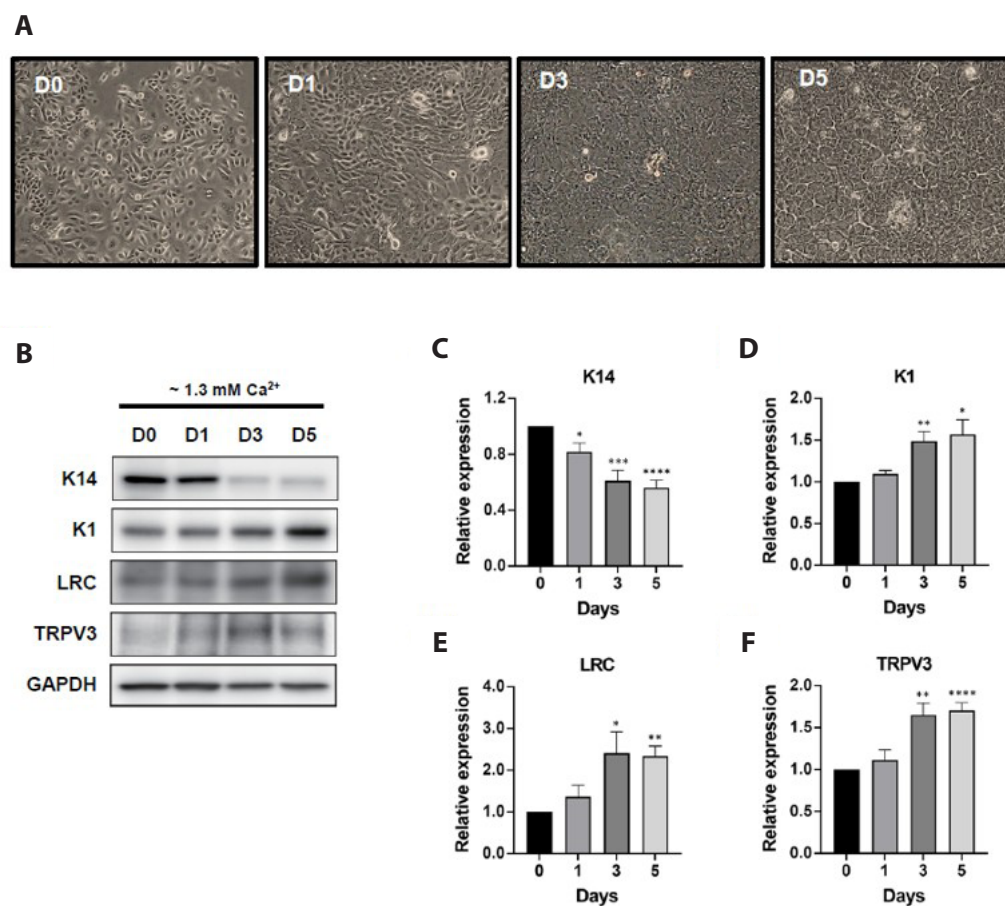


**Fig. 1. Increased expression of TRPV3 in differentiating primary human keratinocytes.** (A) Representative phase contrast images (200× magnification) of keratinocytes during the differentiation process from Day 0 to Day 5 in a high-calcium (> 1.3 mM Ca<sup>2+</sup>) medium. (B) Representative immunoblot results showing changes in K14, K1, LRC, TRPV3, and GAPDH expression during keratinocyte differentiation. GAPDH was used as a loading control. (C) The basal marker K14 significantly decreased over time (\*p = 0.01, \*\*\*p = 0.0002, \*\*\*\*p < 0.0001 vs. Day 0). (D) The early differentiation marker K1 showed a significant increase (\*p = 0.03, \*\*p = 0.01 vs. Day 0). (E) The late differentiation marker LRC exhibited a significant rise (\*p = 0.03, \*\*p = 0.001 vs. Day 0). (F) TRPV3 levels markedly increased after Day 1 (\*\*p = 0.002, \*\*\*\*p < 0.0001 vs. Day 0). Data are presented as mean ± SEM from three independent experiments. Statistical significance was determined using one-way ANOVA followed by Dunnett's multiple comparisons test. TRPV3, transient receptor potential vanilloid 3; K14, keratin 14; K1, keratin 1; LRC, loricrin.

tained at  $20^{\circ}\text{C} \pm 1^{\circ}\text{C}$  and  $50\% \pm 5\%$  humidity. Barrier recovery was calculated using the formula: % barrier recovery = [(TEWL at 0 h – average TEWL of treated group at indicated time point) / (TEWL at 0 h – average TEWL of normal group at indicated time point)]  $\times 100$  [37].

## Statistical analysis

The data are presented as the mean  $\pm$  standard error of the mean (SEM). The statistical significance between each group was determined using either a one-way or two-way analysis of variance (ANOVA).

## RESULTS

### Increased TRPV3 expression and activity during keratinocyte differentiation

Undifferentiated primary human keratinocytes (Day 0, D0) displayed uniform polygonal shapes, which became increasingly flattened by Day 3 (D3) and Day 5 (D5) following calcium-

induced differentiation (Fig. 1A). By D5, the cells exhibited more distinct boundaries, characteristic of terminal keratinocyte differentiation [38–40]. Immunoblot analysis revealed a dynamic pattern of differentiation markers and TRPV3 expression throughout this process. K14 levels dropped sharply by D3 (Fig. 1B, C). Conversely, both K1 and LRC showed significant increases by D3 and maintained elevated levels through D5 (Fig. 1D, E). Notably, TRPV3 expression significantly increased on D3 and remained elevated by D5 (Fig. 1F).

The TRPV3 current ( $I_{\text{TRPV3}}$ ), activated by  $200 \mu\text{M}$  2-APB, was measured using the w-c patch clamp technique (Fig. 2). Representative current trace recordings demonstrate the differential  $I_{\text{TRPV3}}$  responses between undifferentiated and differentiated keratinocytes (Fig. 2A, C). The corresponding I-V relationships (at time points indicated by black arrowheads) show minimal  $I_{\text{TRPV3}}$  in D0 cells (Fig. 2B) but pronounced outwardly rectifying  $I_{\text{TRPV3}}$  in D5 cells (Fig. 2D), with ruthenium red (RR) inhibition being more prominent at negative voltages, consistent with known TRPV3 properties [27]. Comparing the expression of functional TRPV3, the current density of  $I_{\text{TRPV3}}$ , normalized to plasma membrane area (pA/pF), showed a tendency to increase on D3 and became statistically significant on D5 (Fig. 2E).

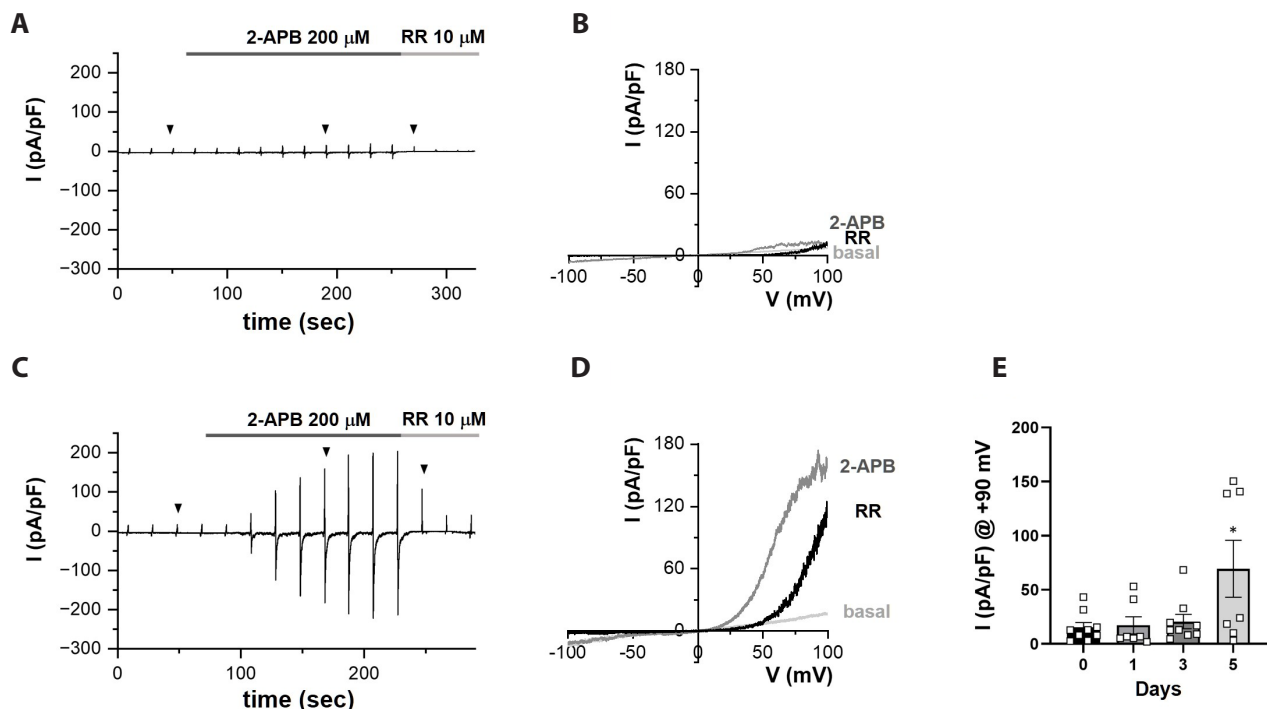


**Fig. 2. Increased functional expression of TRPV3 during keratinocyte differentiation.** (A) Representative current trace recording of primary human keratinocytes on Day 0. TRPV3 was activated with  $200 \mu\text{M}$  2-APB, and RR was applied at the end to confirm the TRPV3 current ( $I_{\text{TRPV3}}$ ). (B) Related I-V relationship curve (black arrow in A) at baseline, after 2-APB application, and following RR treatment. (C) Representative current trace recording of primary human keratinocytes on Day 5. Note the increased  $I_{\text{TRPV3}}$  activated by 2-APB. (D) Related I-V relationship curve (black arrow in C) at baseline, after 2-APB application, and following RR treatment on Day 5. (E) The average current amplitude of 2-APB-elicited  $I_{\text{TRPV3}}$  at  $+90 \text{ mV}$  from Day 0 to 5 (\* $p = 0.03$  vs. Day 0). Data are presented as mean  $\pm$  SEM ( $n = 9$  for D0,  $n = 7$  for D1,  $n = 9$  for D3, and  $n = 7$  for D5). Statistical significance was determined using one-way ANOVA followed by Dunnett's multiple comparisons test. TRPV3, transient receptor potential vanilloid 3; 2-APB, 2-aminoethoxydiphenyl borate; RR, ruthenium red.

To elucidate the implications of upregulated TRPV3 during differentiation, we assessed  $[Ca^{2+}]_i$  levels using Fura-2 fluorescence ratio ( $F_{340/380}$ ) imaging (Fig. 3). Fig. 3A depicts the time-course changes in  $F_{340/380}$  in response to TRPV3 agonists (carvacrol and 2-APB) in primary human keratinocytes at different stages of differentiation. A significant elevation in basal  $F_{340/380}$  was observed on D1 and D3 compared to D0 (Fig. 3B). Interestingly, D5 keratinocytes exhibited basal  $F_{340/380}$  lower than the control.

Upon examination of  $[Ca^{2+}]_i$  levels in response to TRPV3 agonists, we observed an increase of  $[Ca^{2+}]_i$  across all differentiation stages. TRPV3 agonists significantly increased the difference between the peak levels and the average basal levels ( $\Delta F_{340/380}$ ) (Fig. 3C). This analysis revealed that while D5 keratinocytes exhibited significantly lower basal  $[Ca^{2+}]_i$  levels, their net increase in response to TRPV3 activation was comparable to that of D0 keratinocytes. This suggests that while basal  $[Ca^{2+}]_i$  is reduced in fully differentiated keratinocytes, their TRPV3 channels maintain a high capacity for agonist-induced calcium influx.

These results indicate a dynamic regulation of TRPV3 function throughout keratinocyte differentiation, with a potential dissociation between TRPV3 expression, basal  $[Ca^{2+}]_i$ , and agonist-induced calcium influx in the terminal stages.

### Effects of TRPV3 agonists and antagonist on keratinocyte differentiation

To elucidate the role of TRPV3 activation in keratinocyte differentiation, we treated primary human keratinocytes with either a TRPV3 agonist cocktail (2-APB + carvacrol) or a TRPV3 antagonist (RR) and compared the results to a control group treated with the vehicle only.

Inhibition of TRPV3 with RR significantly impeded keratinocyte differentiation. This was evidenced by the sustained expression of K14, a marker of basal keratinocytes, by D5 in the RR-treated group (Fig. 4A, B). The expression level of K1 in RR-treated cells remained relatively constant throughout the differentiation period, showing only a slight increase at D5 without the significant upregulation typically seen during differentiation (Fig. 4A, C). Notably, the increase in TRPV3 expression normally seen during differentiation was absent in RR-treated cells (Fig. 4A, D).

Conversely, treatment with TRPV3 agonists accelerated the differentiation process. This was characterized by a more rapid and pronounced decrease in K14 expression (Fig. 4E, F) and an earlier upregulation of K1, evident as early as D1 (Fig. 4E, G). Quantitative analysis normalized to GAPDH revealed that K1 expression peaked at D1 and gradually decreased thereafter, showing a significant reduction by D5 (Fig. 4G). Intriguingly, TRPV3 expression decreased as differentiation progressed in the presence of TRPV3 agonists (Fig. 4E, H), contrasting with the pattern observed in control conditions.

### Evaluation of TRPV3 modulator on skin barrier recovery

Proper differentiation and cornification of epidermal keratinocytes are crucial for skin barrier formation. To assess the potential of TRPV3 modulators in promoting skin barrier recovery from mechanical damage or clinically relevant conditions, we utilized a tape-stripping barrier disruption model in mice. We applied two different concentrations of TRPV3 agonist cocktails and an antagonist to the tape-stripped mouse back skin and compared the rate of TEWL recovery over 72 h.

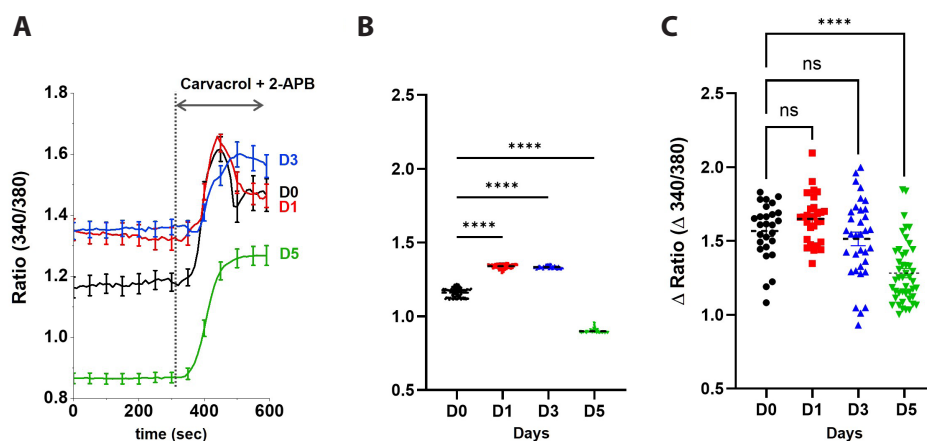


**Fig. 3. Intracellular calcium concentration increases during keratinocyte differentiation.** (A) Time-course of Fura-2 fluorescence ratio (340/380 nm) changes in response to TRPV3 agonists (carvacrol + 2-APB) in primary human keratinocytes, showing D0 (black), D1 (red), D3 (blue), and D5 (green) of differentiation. (B) Quantification of basal intracellular free calcium levels ( $[Ca^{2+}]_i$ ) during keratinocyte differentiation. (C) The net increase in Fura-2 ratio ( $\Delta$ 340/380) calculated by subtracting the average basal  $[Ca^{2+}]_i$  levels from the peak  $[Ca^{2+}]_i$  levels induced by TRPV3 agonists. Data are presented as mean  $\pm$  SEM from each experiment including individual Fura-2 ratio values from 100 cells per group. \*\*\*\* $p$  < 0.0001 vs. D0. Statistical significance was determined using two-way ANOVA followed by Dunnett's multiple comparisons test. TRPV3, transient receptor potential vanilloid 3; 2-APB, 2-aminoethoxydiphenyl borate; ns, not significant.

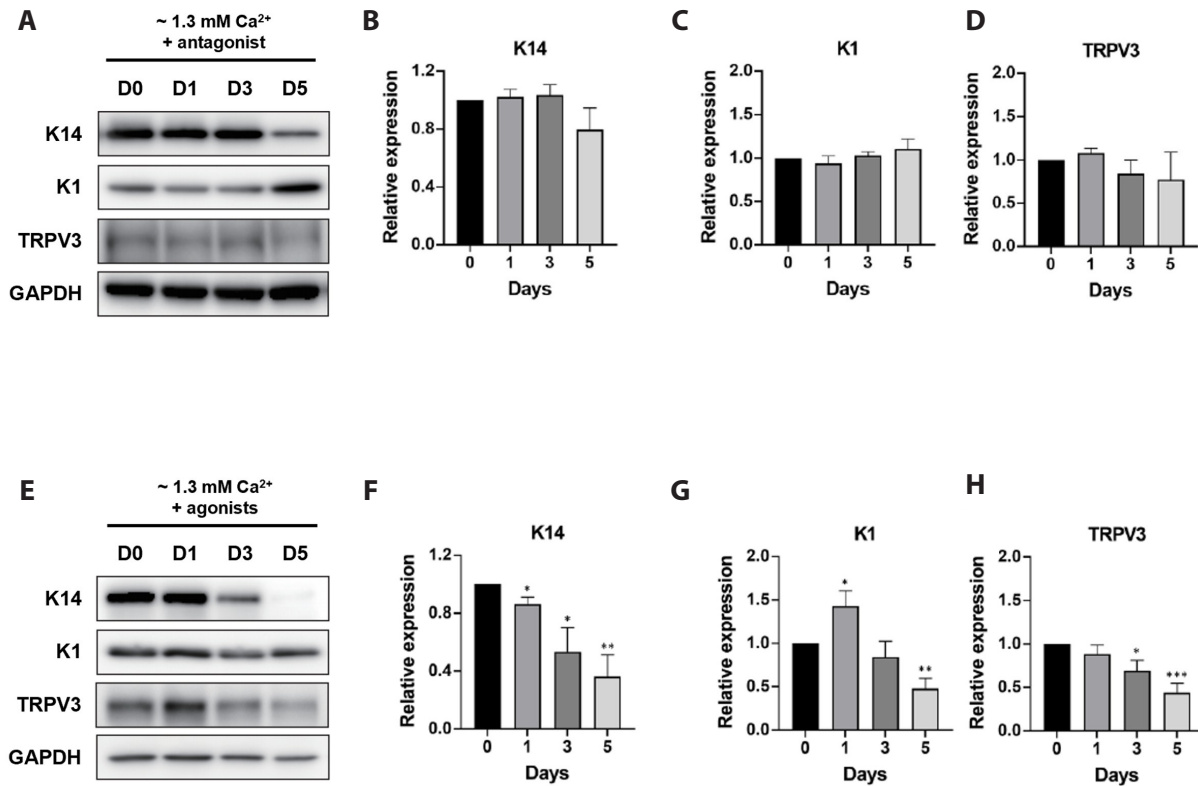


**Fig. 4. Distinct progression of differentiation in keratinocytes with TRPV3 modulation.** (A) Representative immunoblot results showing changes in K14, K1, and TRPV3 expression during keratinocyte differentiation with TRPV3 antagonist (10  $\mu$ M RR) treatment. GAPDH was used as a loading control. (B–D) Quantification of protein expression in RR-treated keratinocytes: (B) K14, (C) K1, and (D) TRPV3. Note that the expression of all proteins remained unchanged throughout the differentiation process. (E) Representative immunoblot results showing changes in K14, K1, and TRPV3 expression during keratinocyte differentiation with TRPV3 agonist cocktail (300  $\mu$ M carvacrol + 30  $\mu$ M 2-APB) treatment. GAPDH was used as a loading control. (F–H) Quantification of protein expression in agonist-treated keratinocytes: (F) K14 showed a marked decrease, (G) K1 significantly increased on Day 1 but dramatically decreased afterward, and (H) TRPV3 levels decreased significantly. Data are presented as mean  $\pm$  SEM from at least three independent experiments. \* $p$  < 0.05, \*\* $p$  < 0.01, \*\*\* $p$  < 0.001 vs. D0. Statistical significance was determined using one-way ANOVA followed by Dunnett's multiple comparisons test. TRPV3, transient receptor potential vanilloid 3; K14, keratin 14; K1, keratin 1; RR, ruthenium red; 2-APB, 2-aminoethoxydiphenyl borate.

After 72 h post-tape-stripping, macroscopic examination of the treated areas revealed noticeable differences in skin appearance. The vehicle-treated group (Fig. 5A) showed typical signs of barrier disruption, with visible redness and scaling. Interestingly, the group treated with the moderate concentration of TRPV3 agonists (300  $\mu$ M carvacrol + 30  $\mu$ M 2-APB) exhibited markedly improved barrier recovery (Fig. 5B). The skin appeared less inflamed and more normalized compared to the vehicle control, suggesting enhanced healing and barrier restoration. In contrast, the higher concentration of TRPV3 agonists (3,000  $\mu$ M carvacrol + 300  $\mu$ M 2-APB) resulted in visibly worse skin condition (Fig. 5C). The treated area showed signs of increased inflammation and erythema, indicating that excessive TRPV3 activation may exacerbate skin barrier dysfunction and inflammatory responses. The group treated with the TRPV3 antagonist RR (10  $\mu$ M) showed barrier recovery comparable to the vehicle control, with no apparent improvement or worsening of the skin condition (Fig. 5D).

Histological analysis substantiated the macroscopic observations. H&E staining of skin sections at 200 $\times$  and 400 $\times$  magnification demonstrated that the moderate concentration of TRPV3 agonists encouraged a more organized epidermal structure and enhanced barrier recovery. Conversely, the higher agonist concentration resulted in indications of excessive inflammation, increased epidermal thickness, and disrupted epidermal structure (Fig. 5A–D, middle and lower rows). Notably, the high-concentration treatment showed significant inflammatory cell infiltration, as highlighted in the 1,000 $\times$  magnification inset (Fig. 5C, bottom row).

Quantitative analysis of inflammatory cell infiltration further validated the histological observations (Fig. 5E). The high-concentration TRPV3 agonist group showed a significant increase in inflammatory cell numbers compared to the vehicle control ( $p$  < 0.0001). Interestingly, both the moderate concentration TRPV3 agonist group and the TRPV3 antagonist group showed no statistically significant difference in inflammatory cell infiltration

## 72hrs after the tape-stripping

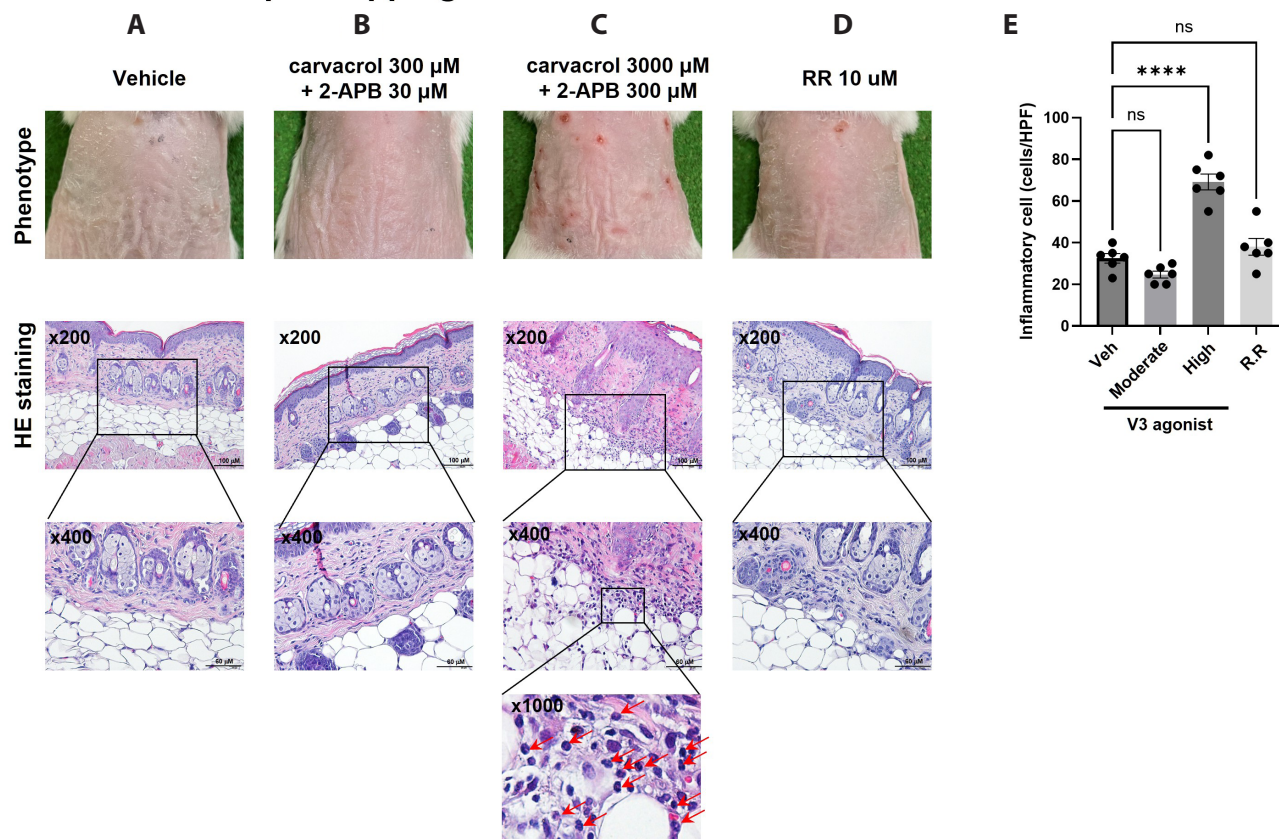


**Fig. 5. Modulation of TRPV3 affects epidermal barrier recovery and inflammation in murine dorsal skin after tape-stripping.** 72 h after tape-stripping, mouse dorsal skin was examined macroscopically and histologically following different treatments. (A-D) The top panels show the macroscopic appearance of mouse dorsal skin. The bottom panels present corresponding hematoxylin & eosin (H&E) staining of skin sections at 200 $\times$  and 400 $\times$  magnification. (A) The vehicle control (0.02% DMSO) shows typical features of barrier disruption. (B) Moderate concentration TRPV3 agonist (300  $\mu$ M carvacrol + 30  $\mu$ M 2-APB) exhibits improved skin condition macroscopically; histologically demonstrates enhanced barrier recovery with a more organized epidermal structure. (C) High concentration TRPV3 agonist (3,000  $\mu$ M carvacrol + 300  $\mu$ M 2-APB) shows increased erythema macroscopically; histologically reveals increased epidermal thickness and significant inflammatory cell infiltration (the infiltrated inflammatory cells are indicated by red arrows in the inset, 1,000 $\times$  magnification). (D) TRPV3 antagonist (10  $\mu$ M RR) appears similar to the vehicle control both macroscopically and histologically. (E) Quantification of inflammatory cell infiltration in H&E-stained skin sections 72 h after tape-stripping and treatment. Data are presented as mean  $\pm$  SEM of cells per high-power field (HPF) from three independent experiments. \*\*\*\* $p$  < 0.0001 vs. the vehicle control. TRPV3, transient receptor potential vanilloid 3; DMSO, dimethyl sulfoxide; 2-APB, 2-aminoethoxydiphenyl borate; RR, ruthenium red; ns, not significant.

compared to the control.

To further assess the impact of TRPV3 modulation on skin barrier function, we measured TEWL over a 72-h period following tape-stripping (Fig. 6). The group treated with the relatively moderate concentrations of TRPV3 agonists (carvacrol 300  $\mu$ M and 2-APB 30  $\mu$ M) showed a significantly improved barrier recovery rate compared to all other groups, particularly noticeable in the early phase of recovery (1–9 h post-tape-stripping,  $p$  < 0.001). On the contrary, the group treated with a high concentration of TRPV3 agonists (3,000  $\mu$ M carvacrol and 2-APB 300  $\mu$ M) exhibited hindered barrier recovery, particularly noticeable during the initial hours (1–6 hours,  $p$  < 0.01 compared to the vehicle). The group treated with TRPV3 antagonist (RR, 10  $\mu$ M) exhibited a barrier recovery profile similar to that of the vehicle control.

## DISCUSSION

Key findings of our study are: 1) increased TRPV3 expression and higher  $I_{TRPV3}$  and agonist-induced  $[Ca^{2+}]_i$  changes in differentiating keratinocytes; 2) augmentation of differentiation markers in TRPV3 agonist-treated keratinocytes; 3) enhanced recovery of the murine skin barrier by moderate concentrations of TRPV3 agonists, while inflammatory changes by higher levels of agonists.

Our *in vitro* experiments with primary human keratinocytes revealed a dynamic relationship between TRPV3 expression and keratinocyte differentiation (Fig. 1). The physiological role of TRPV3 in mouse keratinocytes was previously reported in TRPV3-KO mice that showed defective epidermal barrier formation [26]. Mechanistically, it was suggested that the activation of TRPV3 *in vivo* may lead to an increase in  $Ca^{2+}$ -dependent pro-

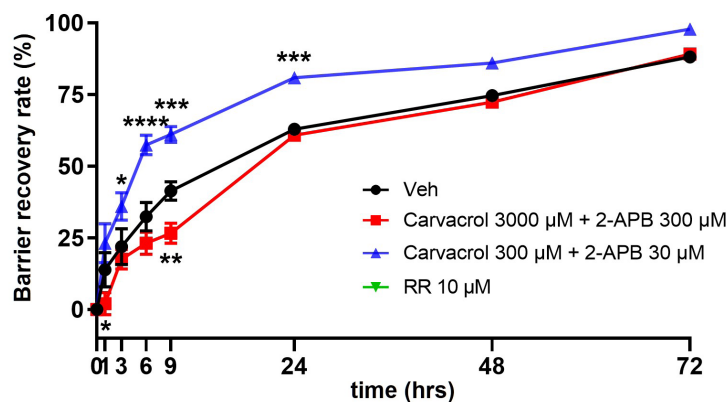


**Fig. 6. TRPV3 modulation influences barrier recovery rate after tape-stripping in mice.** Transepidermal water loss (TEWL) measurements showing barrier recovery rates at 0, 1, 3, 6, 9, 24, 48, and 72 h after tape-stripping. The moderate concentration TRPV3 agonist group (300  $\mu$ M carvacrol + 30  $\mu$ M 2-APB, blue triangles) showed significantly enhanced barrier recovery, particularly in the early phase (1–9 h), compared to the vehicle control (black circles). The high-concentration agonist group (3,000  $\mu$ M carvacrol + 300  $\mu$ M 2-APB, red squares) demonstrated impaired barrier recovery, especially in the initial hours (1–6 h). The TRPV3 antagonist group (10  $\mu$ M RR, green inverted triangles) showed no significant difference from the control. \* $p < 0.05$ , \*\* $p < 0.01$ , \*\*\* $p < 0.001$ , \*\*\*\* $p < 0.0001$  vs. the vehicle control. Data are presented as mean  $\pm$  SEM. For TEWL measurements, mice were sequentially sacrificed for histological analysis at each time point, with initial  $n = 12$  per group at 0 h and final  $n = 5$  per group at 72 h. Statistical significance was determined using two-way ANOVA followed by Dunnett's multiple comparisons test. TRPV3, transient receptor potential vanilloid 3; 2-APB, 2-aminoethoxydiphenyl borate; RR, ruthenium red.

duction/shedding/release of TGF- $\alpha$  or other EGFR ligands and an elevation of transglutaminase activity, which leads to terminal differentiation of keratinocytes. Our data provide additional evidence for the role of TRPV3 in the differentiation of primary human keratinocytes.

Interestingly, we observed that undifferentiated, proliferating keratinocytes showed relatively small  $I_{TRPV3}$  even with the stimulation by 2-APB (Fig. 2A, B). When comparing the levels of TRPV3 protein and  $I_{TRPV3}$ , the expression of TRPV3 was significant on D3 while the amplitude of  $I_{TRPV3}$  became significantly higher on D5. The discrepancy might be due to the time-dependent trafficking to the plasma membrane. Otherwise, the number of keratinocytes examined for the w-c patch clamp study might have been less sufficient to reveal the overall changes of the TRPV3 expression under the  $Ca^{2+}$ -induced differentiation.

Our findings align with previous studies [41,42] in observing an increase in basal  $[Ca^{2+}]_i$  as keratinocyte differentiation progresses (Fig. 3). Interestingly, we noted a sudden decrease in basal  $[Ca^{2+}]_i$  at D5, which represents the terminal differentiation stage, as confirmed by late differentiation markers (Fig. 1). This observation is consistent with previous studies reporting low  $[Ca^{2+}]_i$  in the stratum corneum (SC) [41,42]. While these studies have interpreted the low calcium levels in SC as potentially due to cell death, our D5 cells remained viable and highly responsive to the TRPV3 agonist 2-APB (Fig. 3). These findings suggest a potential regulatory mechanism modulating calcium signaling upon complete differentiation, rather than cell death solely causing low calcium levels. Our results offer new insights into calcium regulation throughout the entire differentiation process, revealing that  $[Ca^{2+}]_i$  levels do not continuously increase in terminal differentiation. Instead, we observed a distinct point where calcium levels

decreased, challenging previous assumptions. This unexpected calcium decrease in fully differentiated keratinocytes may play a yet unknown physiological role in terminal differentiation. The acceleration of differentiation by TRPV3 agonists and its delay by antagonists suggest that TRPV3 may serve as a molecular switch regulating the transition from proliferating to differentiating keratinocytes. This finding has potential implications for disorders characterized by aberrant keratinocyte differentiation, such as psoriasis or ichthyosis [20,43–45]. Furthermore, the increase in both TRPV3 expression and  $I_{TRPV3}$  on D3 and D5 might suggest a self-sustaining role of TRPV3 in the differentiation and maturation of keratinocytes. Consistently, the application of RR, a TRPV3 antagonist, impaired not only the differentiation of keratinocytes but also the TRPV3 upregulation (Fig. 4A–D). However, it has to be also noted that an *in vitro* application of TRPV3 agonists reduced the expression of TRPV3 on D3 and D5 along with the decreased differentiation marker, K1, on D5 following the accelerated increase on D1 (Fig. 4E–H). The results suggested that forced persistent TRPV3 activation might impair the late-phase differentiation or maturation.

Our *in vivo* experiment of TEWL also suggested contrasting effects of TRPV3 agonists depending on their concentration (Fig. 6). Relatively moderate concentrations (300  $\mu$ M carvacrol + 30  $\mu$ M 2-APB) enhanced barrier recovery without significant inflammation, whereas the higher concentrations (3  $\mu$ M carvacrol + 300  $\mu$ M 2-APB) induced inflammatory signs and impaired the barrier recovery. The results suggest the importance of appropriate levels of TRPV3 activators as well as their possibility of therapeutic applications. Interestingly, the TRPV3 antagonist showed no significant effect in our *in vivo* experiments. This may suggest that basal TRPV3 activity is not critical for normal barrier recovery.

ery in the absence of additional stressors, or that compensatory mechanisms involving other calcium channels in keratinocytes come into play when TRPV3 is inhibited. These findings highlight the potential for TRPV3-targeted therapies in skin disorders, despite the challenge of a narrow therapeutic window. This underscores the need for precise modulators and controlled dosing strategies in clinical applications. Future studies examining the effects of co-treatment with TRPV3 antagonists and agonists could provide additional mechanistic insights into the specificity of these responses. Such investigations could help determine whether the beneficial effects of moderate TRPV3 activation and the detrimental effects of excessive activation are both directly mediated through TRPV3, potentially guiding the development of more targeted therapeutic strategies.

Our study demonstrates the critical role of TRPV3 in modulating keratinocyte differentiation, where activation accelerates and inhibition delays the process, underscoring its significance in epidermal homeostasis. We also propose a potential negative feedback mechanism regulating TRPV3 levels during accelerated differentiation, offering insight into the channel's complex dynamics. These findings provide compelling evidence for TRPV3's nuanced role in skin barrier function and suggest that precise modulation of TRPV3 activity could lead to innovative therapeutic approaches in dermatology.

## FUNDING

This research was mainly supported by the National Priority Research Centre Program Grant (NRF-2021R1A6A1A03038865). It was also partially supported by the Korea Health Technology R&D Project through the Korea Health Industry Development Institute (KHIDI), funded by the Ministry of Health & Welfare, Republic of Korea [grant number HP20C0199].

## ACKNOWLEDGEMENTS

None.

## CONFLICTS OF INTEREST

The authors declare no conflicts of interest.

## REFERENCES

- Sun TT, Green H. Differentiation of the epidermal keratinocyte in cell culture: formation of the cornified envelope. *Cell*. 1976;9:511-521.
- Menon GK, Grayson S, Elias PM. Ionic calcium reservoirs in mammalian epidermis: ultrastructural localization by ion-capture cytochemistry. *J Invest Dermatol*. 1985;84:508-512.
- Hennings H, Michael D, Cheng C, Steinert P, Holbrook K, Yuspa SH. Calcium regulation of growth and differentiation of mouse epidermal cells in culture. *Cell*. 1980;19:245-254.
- Pillai S, Bikle DD, Hincenbergs M, Elias PM. Biochemical and morphological characterization of growth and differentiation of normal human neonatal keratinocytes in a serum-free medium. *J Cell Physiol*. 1988;134:229-237.
- Yuspa SH, Kilkenny AE, Steinert PM, Roop DR. Expression of murine epidermal differentiation markers is tightly regulated by restricted extracellular calcium concentrations in vitro. *J Cell Biol*. 1989;109:1207-1217.
- Nemes Z, Steinert PM. Bricks and mortar of the epidermal barrier. *Exp Mol Med*. 1999;31:5-19.
- Elias PM. Stratum corneum defensive functions: an integrated view. *J Invest Dermatol*. 2005;125:183-200.
- Xu H, Ramsey IS, Kotecha SA, Moran MM, Chong JA, Lawson D, Ge P, Lilly J, Silos-Santiago I, Xie Y, DiStefano PS, Curtis R, Clapham DE. TRPV3 is a calcium-permeable temperature-sensitive cation channel. *Nature*. 2002;418:181-186.
- Peier AM, Reeve AJ, Andersson DA, Moqrich A, Earley TJ, Hergarden AC, Story GM, Colley S, Hogenesch JB, McIntyre P, Bevan S, Patapoutian A. A heat-sensitive TRP channel expressed in keratinocytes. *Science*. 2002;296:2046-2049.
- Smith GD, Gunthorpe MJ, Kelsell RE, Hayes PD, Reilly P, Facer P, Wright JE, Jerman JC, Walhin JP, Ooi L, Egerton J, Charles KJ, Smart D, Randall AD, Anand P, Davis JB. TRPV3 is a temperature-sensitive vanilloid receptor-like protein. *Nature*. 2002;418:186-190.
- Chung MK, Lee H, Mizuno A, Suzuki M, Caterina MJ. 2-aminoethoxydiphenyl borate activates and sensitizes the heat-gated ion channel TRPV3. *J Neurosci*. 2004;24:5177-5182.
- Xu H, Delling M, Jun JC, Clapham DE. Oregano, thyme and clove-derived flavors and skin sensitizers activate specific TRP channels. *Nat Neurosci*. 2006;9:628-635.
- Cao X, Yang F, Zheng J, Wang K. Intracellular proton-mediated activation of TRPV3 channels accounts for the exfoliation effect of  $\alpha$ -hydroxyl acids on keratinocytes. *J Biol Chem*. 2012;287:25905-25916.
- Chung MK, Lee H, Mizuno A, Suzuki M, Caterina MJ. TRPV3 and TRPV4 mediate warmth-evoked currents in primary mouse keratinocytes. *J Biol Chem*. 2004;279:21569-21575.
- Moqrich A, Hwang SW, Earley TJ, Petrus MJ, Murray AN, Spencer KS, Andahazy M, Story GM, Patapoutian A. Impaired thermosensation in mice lacking TRPV3, a heat and camphor sensor in the skin. *Science*. 2005;307:1468-1472.
- Huang SM, Lee H, Chung MK, Park U, Yu YY, Bradshaw HB, Coulombe PA, Walker JM, Caterina MJ. Overexpressed transient receptor potential vanilloid 3 ion channels in skin keratinocytes modulate pain sensitivity via prostaglandin E2. *J Neurosci*. 2008;28:13727-13737. Erratum in: *J Neurosci*. 2009;29:29.
- Mandadi S, Sokabe T, Shibasaki K, Katanosaka K, Mizuno A, Moqrich A, Patapoutian A, Fukumi-Tominaga T, Mizumura K, Tominaga M. TRPV3 in keratinocytes transmits temperature information to sensory neurons via ATP. *Pflugers Arch*. 2009;458:1093-1102.
- Yoshioka T, Imura K, Asakawa M, Suzuki M, Oshima I, Hirasawa T,

- Sakata T, Horikawa T, Arimura A. Impact of the Gly573Ser substitution in TRPV3 on the development of allergic and pruritic dermatitis in mice. *J Invest Dermatol.* 2009;129:714-722.
19. Zhao J, Munanairi A, Liu XY, Zhang J, Hu L, Hu M, Bu D, Liu L, Xie Z, Kim BS, Yang Y, Chen ZF. PAR2 mediates itch via TRPV3 signaling in keratinocytes. *J Invest Dermatol.* 2020;140:1524-1532.
  20. Seo SH, Kim S, Kim SE, Chung S, Lee SE. Enhanced thermal sensitivity of TRPV3 in keratinocytes underlies heat-induced pruritogen release and pruritus in atopic dermatitis. *J Invest Dermatol.* 2020;140:2199-2209.e6.
  21. Han Y, Luo A, Kamau PM, Takomthong P, Hu J, Boonyarat C, Luo L, Lai R. A plant-derived TRPV3 inhibitor suppresses pain and itch. *Br J Pharmacol.* 2021;178:1669-1683.
  22. Kim JC, Kim HB, Shim WS, Kwak IS, Chung BY, Kang SY, Park CW, Kim HO. Activation of transient receptor potential vanilloid-3 channels in keratinocytes induces pruritus in humans. *Acta Derm Venereol.* 2021;101:adv00517.
  23. Lei J, Yoshimoto RU, Matsui T, Amagai M, Kido MA, Tominaga M. Involvement of skin TRPV3 in temperature detection regulated by TMEM79 in mice. *Nat Commun.* 2023;14:4104.
  24. Denda M, Sokabe T, Fukumi-Tominaga T, Tominaga M. Effects of skin surface temperature on epidermal permeability barrier homeostasis. *J Invest Dermatol.* 2007;127:654-659. Erratum in: *J Invest Dermatol.* 2007;127:733.
  25. Asakawa M, Yoshioka T, Matsutani T, Hikita I, Suzuki M, Oshima I, Tsukahara K, Arimura A, Horikawa T, Hirasawa T, Sakata T. Association of a mutation in TRPV3 with defective hair growth in rodents. *J Invest Dermatol.* 2006;126:2664-2672.
  26. Borb r  I, Lisztes E, T th BI, Czifra G, Ol h A, Sz llosi AG, Szentandr ssy N, N n si PP, P ter Z, Paus R, Kov cs L, B r  T. Activation of transient receptor potential vanilloid-3 inhibits human hair growth. *J Invest Dermatol.* 2011;131:1605-1614.
  27. Cheng X, Jin J, Hu L, Shen D, Dong XP, Samie MA, Knoff J, Eisinger B, Liu ML, Huang SM, Caterina MJ, Dempsey P, Michael LE, Dlugosz AA, Andrews NC, Clapham DE, Xu H. TRP channel regulates EGFR signaling in hair morphogenesis and skin barrier formation. *Cell.* 2010;141:331-343.
  28. Wang Y, Li H, Xue C, Chen H, Xue Y, Zhao F, Zhu MX, Cao Z. TRPV3 enhances skin keratinocyte proliferation through EGFR-dependent signaling pathways. *Cell Biol Toxicol.* 2021;37:313-330.
  29. Yamanoi Y, Lei J, Takayama Y, Hosogi S, Marunaka Y, Tominaga M. TRPV3-ANO1 interaction positively regulates wound healing in keratinocytes. *Commun Biol.* 2023;6:88.
  30. Lai-Cheong JE, Sethuraman G, Ramam M, Stone K, Simpson MA, McGrath JA. Recurrent heterozygous missense mutation, p.Gly573Ser, in the TRPV3 gene in an Indian boy with sporadic Olmsted syndrome. *Br J Dermatol.* 2012;167:440-442.
  31. Lin Z, Chen Q, Lee M, Cao X, Zhang J, Ma D, Chen L, Hu X, Wang H, Wang X, Zhang P, Liu X, Guan L, Tang Y, Yang H, Tu P, Bu D, Zhu X, Wang K, Li R, et al. Exome sequencing reveals mutations in TRPV3 as a cause of Olmsted syndrome. *Am J Hum Genet.* 2012;90:558-564.
  32. Chiu FP, Salas-Alanis JC, Amaya-Guerra M, Cepeda-Valdes R, McGrath JA, Hsu CK. Novel p.Ala675Thr missense mutation in TRPV3 in Olmsted syndrome. *Clin Exp Dermatol.* 2020;45:796-798.
  33. Zhong W, Hu L, Cao X, Zhao J, Zhang X, Lee M, Wang H, Zhang J, Chen Q, Feng C, Duo L, Wang X, Tang L, Lin Z, Yang Y. Genotype-phenotype correlation of TRPV3-related Olmsted syndrome. *J Invest Dermatol.* 2021;141:545-554.
  34. Sz ll si AG, Vasas N, Angyal  , Kistam s K, N n si PP, Mih ly J, B ke G, Herczeg-Lisztes E, Szegedi A, Kawada N, Yanagida T, Mori T, Kem ny L, B r  T. Activation of TRPV3 regulates inflammatory actions of human epidermal keratinocytes. *J Invest Dermatol.* 2018;138:365-374.
  35. Vasas N, P nz s Z, Kistam s K, N n si PP, Moln r S, Szegedi A, Sz ll si AG, B r  T. Transient receptor potential vanilloid 3 expression is increased in non-lesional skin of atopic dermatitis patients. *Exp Dermatol.* 2022;31:807-813.
  36. Jeriha J, Kolundzic N, Khurana P, Gordon M, Celli A, Mauro TM, Ilic D. Markers for Ca<sup>++</sup>-induced terminal differentiation of keratinocytes in vitro under defined conditions. *Exp Dermatol.* 2020;29:1238-1242.
  37. Alexander H, Brown S, Danby S, Flohr C. Research techniques made simple: transepidermal water loss measurement as a research tool. *J Invest Dermatol.* 2018;138:2295-2300.e1.
  38. Ishida-Yamamoto A, Igawa S. The biology and regulation of corneodesmosomes. *Cell Tissue Res.* 2015;360:477-482.
  39. Ishida-Yamamoto A, Igawa S, Kishibe M, Honma M. Clinical and molecular implications of structural changes to desmosomes and corneodesmosomes. *J Dermatol.* 2018;45:385-389.
  40. Ishida-Yamamoto A, Igawa S, Kishibe M. Molecular basis of the skin barrier structures revealed by electron microscopy. *Exp Dermatol.* 2018;27:841-846.
  41. Celli A, Sanchez S, Behne M, Hazlett T, Gratton E, Mauro T. The epidermal Ca(2+) gradient: measurement using the phasor representation of fluorescent lifetime imaging. *Biophys J.* 2010;98:911-921.
  42. Kumamoto J, Goto M, Nagayama M, Denda M. Real-time imaging of human epidermal calcium dynamics in response to point laser stimulation. *J Dermatol Sci.* 2017;86:13-20.
  43. Yamamoto-Kasai E, Imura K, Yasui K, Shichijou M, Oshima I, Hirasawa T, Sakata T, Yoshioka T. TRPV3 as a therapeutic target for itch. *J Invest Dermatol.* 2012;132:2109-2112.
  44. Martin LS, Fraillon E, Chevalier PF, Fromy B. Hot on the trail of skin inflammation: focus on TRPV1/TRPV3 channels in psoriasis. *IntechOpen.* 2022. doi: 10.5772/intechopen.103792
  45. Nattkemper LA, Tey HL, Valdes-Rodriguez R, Lee H, Mollanazar NK, Albornoz C, Sanders KM, Yosipovitch G. The genetics of chronic itch: gene expression in the skin of patients with atopic dermatitis and psoriasis with severe itch. *J Invest Dermatol.* 2018;138:1311-1317.